



This is a self-archived version of an original article. This version may differ from the original in pagination and typographic details.

Author(s): ALICE Collaboration

Title: System-size dependence of the charged-particle pseudorapidity density at $\sqrt{s}_{\text{NN}} = 5.02$ TeV for pp, p–Pb, and Pb–Pb collisions

Year: 2023

Version: Published version

Copyright: © 2023 European Center of Nuclear Research, ALICE experiment. Published by Elsevier Ltd on behalf of the European Physical Journal Experts Services Unit. All rights reserved.

Rights: CC BY 4.0

Rights url: <https://creativecommons.org/licenses/by/4.0/>

Please cite the original version:

ALICE Collaboration. (2023). System-size dependence of the charged-particle pseudorapidity density at $\sqrt{s}_{\text{NN}} = 5.02$ TeV for pp, p–Pb, and Pb–Pb collisions. Physics Letters B, 845, Article 137730. <https://doi.org/10.1016/j.physletb.2023.137730>



System-size dependence of the charged-particle pseudorapidity density at $\sqrt{s_{NN}} = 5.02 \text{ TeV}$ for pp, p–Pb, and Pb–Pb collisions



ALICE Collaboration*

ARTICLE INFO

Article history:

Received 20 May 2022

Received in revised form 17 January 2023

Accepted 17 January 2023

Available online 4 February 2023

Editor: M. Doser

ABSTRACT

We present the first systematic comparison of the charged-particle pseudorapidity densities for three widely different collision systems, pp, p–Pb, and Pb–Pb, at the top energy of the Large Hadron Collider ($\sqrt{s_{NN}} = 5.02 \text{ TeV}$) measured over a wide pseudorapidity range ($-3.5 < \eta < 5$), the widest possible among the four experiments at that facility. The systematic uncertainties are minimised since the measurements are recorded by the same experimental apparatus (ALICE). The distributions for p–Pb and Pb–Pb collisions are determined as a function of the centrality of the collisions, while results from pp collisions are reported for inelastic events with at least one charged particle at midrapidity. The charged-particle pseudorapidity densities are, under simple and robust assumptions, transformed to charged-particle rapidity densities. This allows for the calculation and the presentation of the evolution of the width of the rapidity distributions and of a lower bound on the Bjorken energy density, as a function of the number of participants in all three collision systems. We find a decreasing width of the particle production, and roughly a smooth ten fold increase in the energy density, as the system size grows, which is consistent with a gradually higher dense phase of matter.

© 2023 European Center of Nuclear Research, ALICE experiment. Published by Elsevier B.V. This is an open access article under the CC BY license (<http://creativecommons.org/licenses/by/4.0/>). Funded by SCOAP³.

1. Introduction

The number of charged particles produced in energetic nuclear collisions is an important indicator for the strong interaction processes that determine the particle production at the sub-nucleonic level. In particular, the production of charged particles is expected to reflect the number of quark and gluon collisions occurring during the initial stages of the reaction. The total number of particles produced also provides information on the energy transfer available from the initial colliding beams to particle production, as a consequence of nuclear stopping [1]. In order to help unravel this complex scenario it is important to compare the particle production amongst collision systems of different sizes over a wide kinematic range.

We present the measured charged-particle pseudorapidity density, $dN_{\text{ch}}/d\eta$, for pp, p–Pb, and Pb–Pb (previously published [2]) collisions at the same collision energy of $\sqrt{s_{NN}} = 5.02 \text{ TeV}$ in the nucleon–nucleon centre-of-mass reference frame. This is, at present, the maximum available energy at CERN's Large Hadron Collider (LHC) for Pb–Pb collisions. The measurements were carried out using ALICE at LHC (for earlier $dN_{\text{ch}}/d\eta$ results see for example Refs. [3–5]). The three studied reactions have different

characteristics probing widely different particle production yields and mechanisms. In Pb–Pb collisions, the total particle yield for central collisions is of the order 10^4 [2], and a strongly coupled plasma of quarks and gluons (sQGP) is formed [6–9], whose collective and transport properties are currently under intense study. On the other hand, pp collisions represent the simplest possible nuclear collision system, where the average total particle production is much smaller (≈ 80 , by integrating the measured distributions), and is to first approximation much less subject to collective effects [10]. The p–Pb system is intermediate to the other reactions, corresponding to the situation where a single nucleon probes the nucleons in a narrow cylinder of the target nucleus. The extent to which p–Pb is governed by the initial state cold nuclear matter of the lead ion or whether collective phenomena in the hot and dense medium play an important role is, at present, a matter under scrutiny by the community [10,11].

In this letter, we compare the three reactions and present the ratios of the charged-particle pseudorapidity density distributions ($dN_{\text{ch}}/d\eta$) of the more complex reactions to the pp distribution. Owing to ALICE's unique large acceptance in pseudorapidity, and using simple and robust assumptions, we transform the measured charged-particle pseudorapidity density distributions into charged-particle rapidity density distributions (dN_{ch}/dy). This allows us to calculate the width of the rapidity distributions as a function of the number of participating nucleons. The parameters of the

* E-mail address: alice-publications@cern.ch.

transformation also allow us to estimate a lower bound on the energy density using the well-known formula from Bjorken [12]. An energy density exceeding the critical energy density of roughly 1 GeV/fm^3 [13] is a necessary condition for the formation of deconfined matter of quarks and gluons, and thus it is of the utmost interest to understand the development of these energy densities across different collision systems.

2. Experimental set-up, data sample, analysis method, systematic uncertainties

A detailed description of the ALICE detector and its performance can be found elsewhere [14,15]. The present analysis uses the Silicon Pixel Detector (SPD) to determine the pseudorapidity densities in the range $-2 < \eta < 2$ and the Forward Multiplicity Detector (FMD) in the ranges $-3.5 < \eta < -1.8$ and $1.8 < \eta < 5$. The V0, comprised of two plastic scintillator discs covering $-3.7 < \eta < -1.7$ (VOC) and $2.8 < \eta < 5.1$ (VOA), and the ZDC, two zero-degree calorimeters located 112.5 m from the interaction point, measurements determine the collision centrality and are used for offline event selection [2].

The results presented are based on data from collisions at a centre-of-mass energy per nucleon pair of $\sqrt{s_{\text{NN}}} = 5.02 \text{ TeV}$ as collected by ALICE during LHC Run 1 (2013) for p-Pb, and during Run 2 (2015) for pp and Pb-Pb. The FMD suffered high levels of background noise during the 2016 p-Pb campaign, due to the high collision rate, and this data is therefore not used for the present analysis. About 10^5 events with a minimum bias trigger requirement [2] were analysed in the centrality range from 0% to 90% and 0% to 100% of the visible cross section for Pb-Pb and p-Pb collisions, respectively. The minimum bias trigger for p-Pb and Pb-Pb collisions in ALICE was defined as a coincidence between the VOA and VOC sides of the V0 detector.

The data from the p-Pb collisions were taken in two beam configurations: one where the lead ion travelled toward positive pseudorapidity and one where it travelled toward negative pseudorapidity. The results from the latter collisions are mirrored around $\eta = 0$. The centre-of-mass frame in p-Pb collisions does not coincide with the laboratory frame, due to the single magnetic field in the LHC, and thus the rapidity of the centre-of-mass is $y_{\text{CM}} = \pm 0.465$ for the two directions, respectively, in the laboratory frame. For this reason, pseudorapidity, calculated with respect to the laboratory frame, is denoted η_{lab} whenever p-Pb results are presented.

Likewise, for the pp collisions, about 10^5 events with coincidence between VOA and VOC and at least one charged particle in $|\eta| < 1$ were analysed. By requiring at least one charged particle at midrapidity, the so-called INEL>0 event class, the systematic uncertainty, related to the absolute normalisation to the full inelastic cross section, is reduced, while still sampling a large fraction ($> 75\%$) of the hadronic cross section [16,17].

The standard ALICE event selection [18] and centrality estimator based on the V0 amplitude [19,20] are used in this analysis. The event selection consists of: a) exclusion of background events using the timing information from the ZDC (for Pb-Pb and p-Pb, e.g., beam-gas interactions) and V0 detectors, b) verification of the trigger conditions, and c) a reconstructed position of the collision (primary vertex). In Pb-Pb collisions, centrality is obtained from the sum amplitude in both V0 detector arrays (VOM). For p-Pb only the amplitude in the array on the lead-going side (VOA or VOC) is used. In Pb-Pb collisions, the 10% most peripheral collisions have substantial contributions from electromagnetic processes and are therefore not included in the results presented here [19].

A primary charged particle is defined as a charged particle with a mean proper lifetime τ larger than 1 cm/c , which is either a) produced directly in the interaction, or b) from decays of particles

with τ smaller than 1 cm/c [21]. All quantities reported here are for primary, charged particles, though “primary” is omitted in the following for brevity.

The analysis method is identical to that of previous publications [2]: the measurement of the charged-particle pseudorapidity density at midrapidity is obtained from counting particle trajectories determined using the two layers of the SPD. The SPD has a lower transverse momentum acceptance of $50 \text{ MeV}/c$, and the yield is extrapolated down to $p_T = 0 \text{ MeV}/c$ via simulations. In the forward regions, the measurement is provided by the analysis of the deposited energy signal in the FMD and a statistical method is employed to calculate the inclusive number of charged particles. A data-driven correction [22], based on separate measurements exploiting displaced collision vertices, is applied to remove the background from secondary particles.

Systematic uncertainty estimations for the midrapidity measurements are detailed elsewhere [2,16,20], and are from background suppression, transverse momentum extrapolation, weak decays, and simulations. The estimates are obtained through variation of thresholds and simulation studies. For pp (p-Pb), the total systematic uncertainty amounts to 1.5% (2.7%) over the whole pseudorapidity range; while for Pb-Pb the total systematic uncertainty is 2.6% at $\eta = 0$ and 2.9% at $|\eta| = 2$. The systematic uncertainty is mostly correlated over pseudorapidity for $|\eta| < 2$, and largely independent of centrality. The uncertainty in the forward region, estimated via variations of thresholds and simulation studies, is the same for all collision systems and is uncorrelated across η , amounting to 6.9% for $\eta > 3.5$ and 6.4% elsewhere within the forward regions [22]. In the figures of this letter, uncorrelated, local in pseudorapidity, systematic uncertainties are indicated by open boxes on the data points, while correlated systematic uncertainties, those that affect the overall scale and typically from event classification and selection, are indicated by filled boxes to the right of the data. The systematic uncertainty on $dN_{\text{ch}}/d\eta$, due to the centrality class definition in Pb-Pb, is estimated to vary from 0.6% for the most central to 9.5% for the most peripheral class [23]. The 80% to 90% centrality class has residual contamination from electromagnetic processes as detailed elsewhere [19], which gives rise to an additional 4% systematic uncertainty in the measurements. No overall systematic uncertainty has been estimated for p-Pb collisions, as the centrality selection in that collision system is inherently difficult to map to the underlying dynamics of the collisions [20].

3. Results

Fig. 1 shows the measured pseudorapidity densities in pp, and in central p-Pb, and the previously published results for Pb-Pb [2] collisions at $\sqrt{s_{\text{NN}}} = 5.02 \text{ TeV}$ for primary particles.

For the 5% most central Pb-Pb collisions $dN_{\text{ch}}/d\eta \approx 2000$ at midrapidity ($\eta = 0$) [2], while for p-Pb collisions the distribution peaks at $dN_{\text{ch}}/d\eta_{\text{lab}} \approx 60$ around $\eta_{\text{lab}} = 3$ in the lead-going direction ($\eta > 0$). For pp collisions with the INEL>0 trigger condition discussed above, $dN_{\text{ch}}/d\eta = 5.7 \pm 0.2$ at midrapidity, consistent with previous results derived from p_T spectra [24].

Fig. 2 shows, as a function of centrality, the measured charged-particle pseudorapidity densities for p-Pb collisions at $\sqrt{s_{\text{NN}}} = 5.02 \text{ TeV}$. The strategy of centrality selection for proton on nucleus reactions is explained elsewhere [20]. The ALICE Collaboration has previously presented $dN_{\text{ch}}/d\eta$ for Pb-Pb collisions at this energy [2].

In Fig. 3, the charged-particle pseudorapidity densities in p-Pb and Pb-Pb reactions are divided by the pp distributions corresponding to the INEL>0 trigger class. The ratio is $r_X = (dN_{\text{ch}}/d\eta|_X)/(dN_{\text{ch}}/d\eta|_{\text{pp}})$, where X labels p-Pb and Pb-Pb collisions, in centrality classes, as a function of pseudorapidity. In

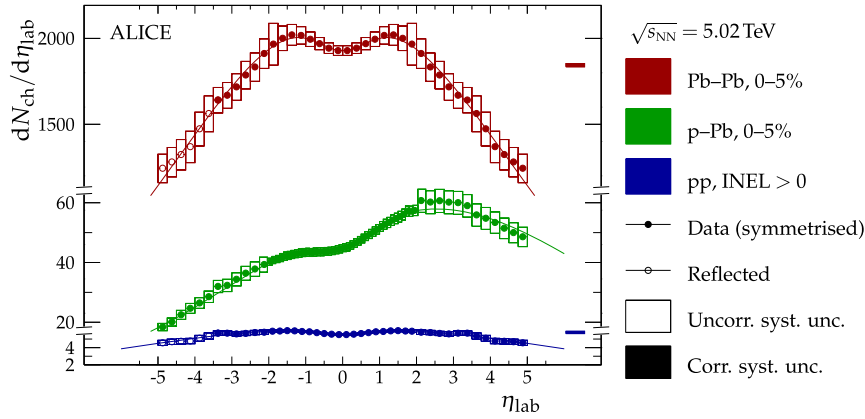


Fig. 1. Charged-particle pseudorapidity density in Pb–Pb [2] and p–Pb for the 5% most central collisions, and for pp collisions with INEL>0 trigger class. For symmetric collision systems (Pb–Pb and pp) the data has been symmetrised around $\eta=0$ and points for $\eta>3.5$ have been reflected around $\eta=0$. The boxes around the points and to the right reflect the uncorrelated and correlated, with respect to pseudorapidity, systematic uncertainty, respectively. The relative correlated, normalisation, uncertainties are evaluated at $dN_{ch}/d\eta|_{\eta=0}$. The lines show fits of Eq. (1) (Pb–Pb and pp) and Eq. (2) (p–Pb) to the data (discussed in Section 4). Please note that the ordinate has been cut twice to accommodate for the very different ranges of the charged-particle pseudorapidity densities.

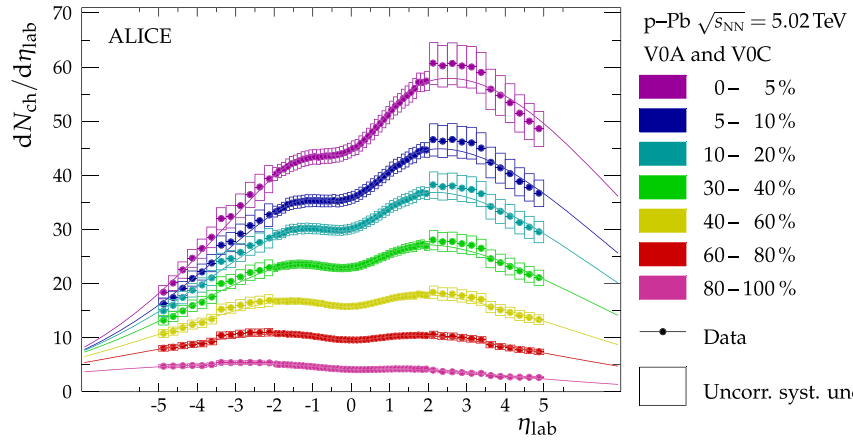


Fig. 2. Charged-particle pseudorapidity density in p–Pb collisions at $\sqrt{s_{NN}} = 5.02$ TeV in seven centrality classes based on the V0A and V0C estimators. The lines are obtained using a fit of a scaled, normal distribution in rapidity Eq. (2) to the data (discussed in Section 4).

the ratios, systematic uncertainties, of common origin, are partially cancelled, and, as an estimate, the magnitude of the resulting systematic uncertainties are given only by the uncertainties in the $dN_{ch}/d\eta|_X$ measurements, since the uncertainties are independent of the collision system. In p–Pb collisions the rapidity of the centre-of-mass is non-zero, which is not taken into account in the ratios. Such a correction would require prior determination of the full Jacobian of the transformation from pseudorapidity to rapidity, which is not possible to perform reliably with the ALICE apparatus.

The ratio of the p–Pb relative to the pp distributions increases with pseudorapidity from the p-going to the Pb-going direction for central collisions, which Brodsky et al. and Adil et al. [25,26] suggest is a sign of scaling of the pp distribution with the increasing number of participants as the lead nucleus is probed by the incident proton, and thus independent proton–nucleon scatterings on the lead-ion side. A similar scaling, however, does not hold for the Pb–Pb reaction. The ratios cannot be obtained by simple scaling of the elementary pp distributions. Instead, the ratio of the Pb–Pb relative to the pp distributions exhibits an enhancement of particle production around midrapidity for the more central collisions which is indicative of the formation of the sQGP [7]. Likewise, r_{pPb} increases for all but the two most peripheral centrality classes as $\eta_{lab} \rightarrow 3$. In Pb–Pb collisions it is seen that the various mechanisms behind the pseudorapidity distributions are more transversely directed than in pp collisions by the increase of r_{pPb} as $|\eta| \rightarrow 0$

4. Rapidity and energy-density dependence on system size and discussion

It has been shown that the charged-particle rapidity density (dN_{ch}/dy) in Pb–Pb collisions, to a good accuracy, follows a normal distribution over the considered rapidity interval ($|y| \lesssim 5$) [2,27]. Those results relied on calculating the average Jacobian $dN_{ch}/dy = \langle J \rangle = \langle \beta \rangle$ using the full p_T spectra, at midrapidity, of charged pions and kaons as well as protons and antiprotons. Here, we use the approximation

$$y \approx \eta - \frac{1}{2} \frac{m^2}{p_T^2} \cos \vartheta,$$

where ϑ is the polar angle of emission, and identify $a = p_T/m$ with an effective ratio of transverse momentum over mass. With this, the effective Jacobian can be written as

$$J'(\eta, a) = \left(1 + \frac{1}{a^2} \frac{1}{\cosh^2 \eta} \right)^{-1/2}.$$

We further make the ansatz that dN_{ch}/dy is normal distributed for symmetric collision systems (pp and Pb–Pb), so that $dN_{ch}/d\eta$ can be parameterised as

$$f(\eta; A, a, \sigma) = J'(\eta, a) A \frac{1}{\sqrt{2\pi}\sigma} \exp \left(-\frac{\eta^2 \{ \eta, a \}}{2\sigma^2} \right), \quad (1)$$

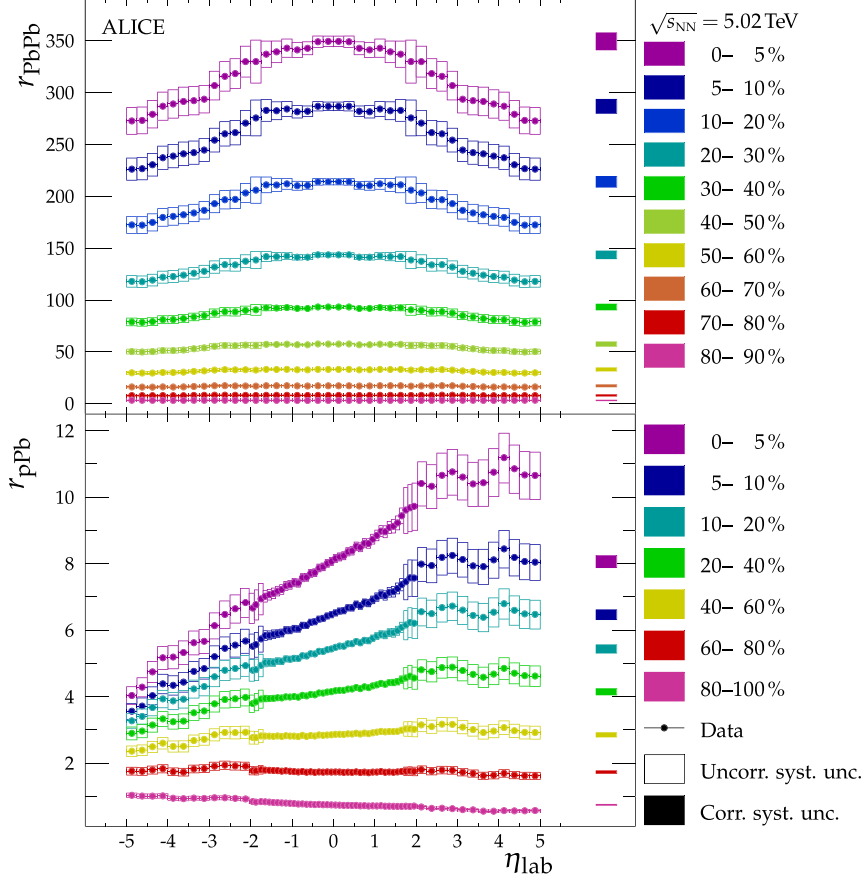


Fig. 3. Ratio r_X of the charged-particle pseudorapidity density in Pb–Pb (top) and p–Pb (bottom) in different centrality classes to the charged-particle pseudorapidity density in pp in INEL>0 event class. Note, for Pb–Pb η_{lab} is the same as the centre-of-mass pseudorapidity.

where A and σ are the total integral and width of the distribution, respectively, and y the rapidity in the centre-of-mass frame. Motivated by the observed approximate linearity of r_{pPb} (see lower panel of Fig. 3), we replace A with $(\alpha y + A)$ for the asymmetric system (p–Pb) and parameterise $dN_{\text{ch}}/d\eta_{\text{lab}}$ as

$$g(\eta; A, a, \alpha, \sigma) = J'(\eta, a) (\alpha y\{\eta, a\} + A) \times \frac{1}{\sqrt{2\pi}\sigma} \exp\left(-\frac{|y\{\eta, a\} - y_{\text{CM}}|^2}{2\sigma^2}\right). \quad (2)$$

The functions f and g defined in Eq. (1) and Eq. (2), respectively, describe the measurements within the measured region with χ^2 per degrees of freedom (ν) in the range of 0.1 to 0.5. The small χ^2/ν values are a consequence of the relatively large uncorrelated systematic uncertainties on the measurements. That is, the charged-particle distributions for pp, p–Pb, and Pb–Pb collisions at $\sqrt{s_{\text{NN}}} = 5.02$ TeV follow a normal distribution in rapidity, with free parameters A , a , σ , and α in the asymmetric case.

The top panel of Fig. 4 shows the best-fit parameter values of the normal width ($\sigma_{dN_{\text{ch}}/dy}$) for all three collision systems as a function of the average number of participating nucleons ($\langle N_{\text{part}} \rangle$) calculated using a Glauber model [28]. The best-fit parameters are found taking statistical and uncorrelated systematic uncertainties into account. The result using the above procedure, for the most central Pb–Pb collisions, is found to be compatible with previous results extracted by unfolding with the mean Jacobian estimated from transverse momentum spectra [2]. The open points (crosses) and dashed lines on the figure are from evaluations of Eq. (1) and Eq. (2), and direct calculations of $\sigma_{dN_{\text{ch}}/dy}$, respectively, using model calculations with EPOS-LHC [29]. EPOS-LHC was chosen as it provides predictions for all three collision systems. The param-

eterisation, in terms of the two functions, of this model calculation generally reproduces the widths of the charged-particle rapidity densities, except in the asymmetric case where a direct evaluation of the standard deviation is less motivated.

The general trend is that the widths decrease as $\langle N_{\text{part}} \rangle$ increases, consistent with the behaviour of the r_{pPb} ratios. Notably, the width of the dN_{ch}/dy distributions in p–Pb and Pb–Pb, for low number of participant nucleons in the collisions, approaches the width of the pp distribution, which, presumably, is dominated by kinematic and phase space constraints.

The lower panel of Fig. 4 shows the dependence of a on the average number of participants. The right-hand ordinate is the same, but multiplied by the average mass $\langle m \rangle = (0.215 \pm 0.001)$ GeV/ c^2 estimated from measurements of identified particles in Pb–Pb collisions at $\sqrt{s_{\text{NN}}} = 2.76$ TeV [30]. To better understand the parameter a , this parameter extracted from the EPOS-LHC calculations, using the above procedure, is also shown in the figure. The dotted lines show the average p_T/m predicted by EPOS-LHC [29]. The EPOS-LHC calculations indicate that the extracted effective transverse momentum to mass ratio a is consistently smaller than the ratio of the average transverse momentum to the average mass. Thus a gives a lower bound on $\langle p_T \rangle / \langle m \rangle$.

We can estimate the energy density that is reached in the collisions as a function of the number of participants for the three systems. A conventional approach is to use the model originally proposed by Bjorken [12] in which the energy density (ε_{Bj}) depends on the rapidity density of particles and the volume of a longitudinal cylinder with cross sectional area determined by the overlap between the colliding partners and length determined by a characteristic particle formation time

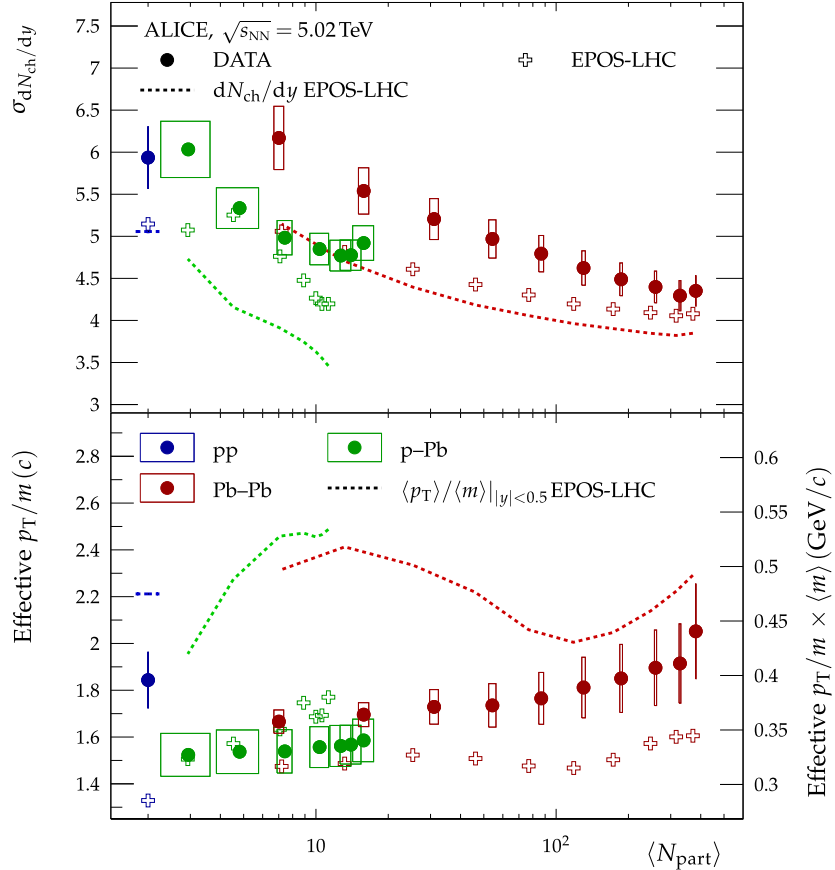


Fig. 4. The width (top) and effective p_{T}/m (bottom) fit parameters as a function of the mean number of participants in pp, p-Pb, and Pb-Pb collisions at $\sqrt{s_{\text{NN}}} = 5.02 \text{ TeV}$. Vertical uncertainties are the standard error on the best-fit parameter values, while horizontal uncertainties reflect the uncertainty on $\langle N_{\text{part}} \rangle$ from the Glauber calculations. Also shown are similar fit parameters from the same parameterisation of EPOS-LHC calculations as well as direct calculations of the standard deviation of the dN_{ch}/dy distributions and the $\langle p_{\text{T}} \rangle / \langle m \rangle$ ratio from the EPOS-LHC calculations.

$$\varepsilon_{\text{Bj}} = \frac{1}{c\tau} \frac{1}{S_{\text{T}}} \left\langle \frac{dE_{\text{T}}}{dy} \right\rangle.$$

Here, $S_{\text{T}} \approx \pi R^2 \approx \pi N_{\text{part}}^{2/3}$ is the transverse area spanned by the participating nucleons, dE_{T}/dy is the transverse-energy rapidity density, and τ is the formation time. While a formation time of $\tau = 1 \text{ fm/c}$ is often assumed, it is left as a free parameter here. With $\langle m_{\text{T}} \rangle = \langle m \rangle \sqrt{1 + (\langle p_{\text{T}} \rangle / \langle m \rangle)^2}$, the transverse-energy rapidity density can be approximated by

$$\left\langle \frac{dE_{\text{T}}}{dy} \right\rangle \approx \langle m_{\text{T}} \rangle \frac{1}{f_{\text{total}}} \frac{dN_{\text{ch}}}{dy} = \langle m \rangle \sqrt{1 + \left(\frac{\langle p_{\text{T}} \rangle}{\langle m \rangle} \right)^2} \frac{1}{f_{\text{total}}} \frac{dN_{\text{ch}}}{dy},$$

where $f_{\text{total}} = 0.55 \pm 0.01$, the ratio of charged particles to all particles [31], accounts for neutral particles not measured in the experiment, and is assumed the same for all collision systems. Substituting the derived dN_{ch}/dy and the effective $a = p_{\text{T}}/m \lesssim \langle p_{\text{T}} \rangle / \langle m \rangle$ results in a lower bound estimate for the Bjorken energy density (ε_{LB})

$$\varepsilon_{\text{Bj}} \tau \geq \varepsilon_{\text{LB}} \tau = \frac{1}{c} \frac{1}{S_{\text{T}}} \langle m \rangle \sqrt{1 + a^2} \frac{1}{f_{\text{total}}} \sqrt{1 + \frac{1}{a^2} \frac{1}{\cosh^2 \eta}} \frac{dN_{\text{ch}}}{d\eta}, \quad (3)$$

where a and $\langle m \rangle$ are as in the top panel of Fig. 4.

The transverse area S_{T} is estimated in a numerical Glauber model [32,33] as shown in Fig. 5. We consider two extremes for the transverse area spanned by the participating nucleons: a) the *exclusive* (or direct) overlap between participating nucleons, \cap and open markers in Fig. 5, and b) the *inclusive* (or full) area of all participating nucleons, \cup and full markers in Fig. 5.

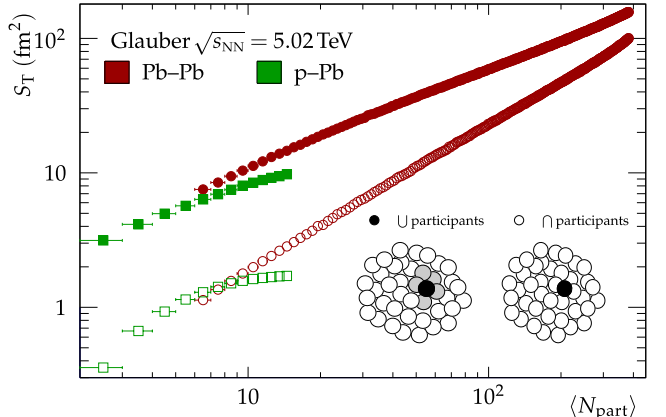


Fig. 5. The transverse area S_{T} as calculated in a numerical Glauber model for two extreme cases: a) only the exclusive overlap of nucleons is considered (\cap , open markers) and b) the inclusive area of participating nucleons contribute (\cup , closed markers) in both p-Pb and Pb-Pb at $\sqrt{s_{\text{NN}}} = 5.02 \text{ TeV}$.

Fig. 6 shows the lower-bound energy density estimate, $\varepsilon_{\text{LB}} \tau \leq \varepsilon_{\text{Bj}} \tau$, as a function of the number of participants, which reaches values between 10 and $20 \text{ GeV}/(\text{fm}^2 c)$ in the most central Pb-Pb collisions. The uncertainties are from standard error propagation of Eq. (3) of uncertainties on the best-fit parameter values, the number of participants, mean mass, and f_{total} . A rise from roughly $1 \text{ GeV}/(\text{fm}^2 c)$ to over $10 \text{ GeV}/(\text{fm}^2 c)$ is observed if the transverse area is assumed to be the inclusive area of participating nucleons. This trend is illustrated by a power-law ($C N_{\text{part}}^p$) fit to the data in

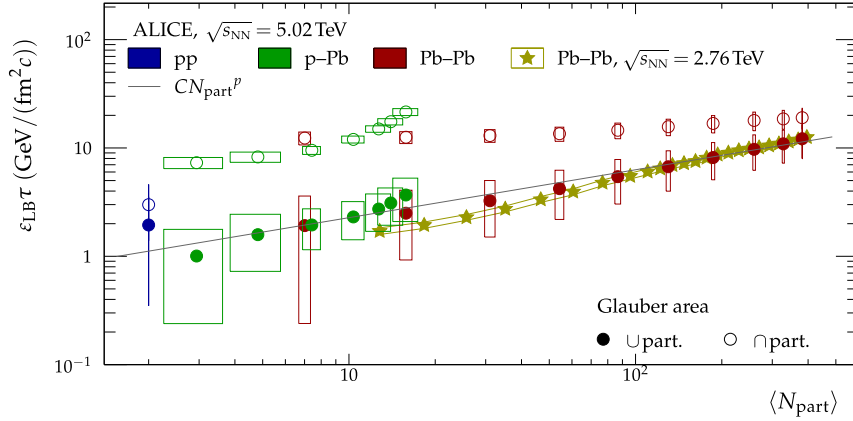


Fig. 6. Estimate of the lower bound on the Bjorken transverse energy density in pp, p-Pb, and Pb-Pb collisions at $\sqrt{s_{\text{NN}}} = 5.02$ TeV, considering the exclusive (\cap , open markers) and inclusive (\cup , full markers) overlap area S_T of the nucleons. The expression CN_{part}^p is fitted to case \cup , and we find $C = (0.8 \pm 0.3)$ GeV/(fm 2c) and $p = 0.44 \pm 0.08$. Also shown is an estimate, via dE_T/dy , of ε_{Bj} from Pb-Pb collisions at $\sqrt{s_{\text{NN}}} = 2.76$ TeV (stars with uncertainty band) [31].

the figure, with the parameter values $C = (0.8 \pm 0.3)$ GeV/(fm 2c) and $p = 0.44 \pm 0.08$. On the other hand, if the transverse area is assumed to be the smaller exclusive overlap area, we observe a substantially larger lower bound on the energy density, but a less dramatic increase with increasing number of participating nucleons. Also shown in the figure are estimates of the Bjorken energy density $\varepsilon_{\text{Bj}} \tau$ for Pb-Pb reactions at $\sqrt{s_{\text{NN}}} = 2.76$ TeV [31]. These results were obtained from measurements of the transverse energy in the collisions and using the inclusive estimate of the transverse area S_T . The trend of the $\sqrt{s_{\text{NN}}} = 5.02$ TeV results is similar to these earlier results. Bearing in mind that for the largest LHC collision energy we show a lower bound estimate of the energy density in Fig. 6, we find a likely overall increase in the energy density from $\sqrt{s_{\text{NN}}} = 2.76$ TeV to 5.02 TeV.

5. Summary and conclusions

We have measured the charged particle pseudorapidity density in pp, p-Pb, and Pb-Pb collisions at $\sqrt{s_{\text{NN}}} = 5.02$ TeV over the widest possible pseudorapidity range available at the LHC. The distributions were determined using the same experimental apparatus and methods, and systematic uncertainties have been minimised to within the capabilities of the set-up. While the particle production in central Pb-Pb collisions clearly exhibits an enhancement as compared to pp collisions, particle production in p-Pb collisions is consistent with dominantly incoherent nucleon-nucleon collisions. By transforming the measured pseudorapidity distributions to rapidity distributions we have obtained systematic trends for the width of the rapidity distributions and a lower bound on the energy density, which shows a clear scaling behaviour as a function of the average number of participant nucleons. The decreasing width of the deduced rapidity distributions with increasing participant number suggests that the kinematic spread of particles, including longitudinal degrees of freedom, is reduced due to interactions in the early stages of the collisions. This is also reflected in the accompanying growth of the energy density. Both observations are consistent with the gradual establishment of a high-density phase of matter with increasing size of the collision domain.

Declaration of competing interest

The authors declare that they have no known competing financial interests or personal relationships that could have appeared to influence the work reported in this paper.

Acknowledgements

The ALICE Collaboration would like to thank all its engineers and technicians for their invaluable contributions to the construction of the experiment and the CERN accelerator teams for the outstanding performance of the LHC complex. The ALICE Collaboration gratefully acknowledges the resources and support provided by all Grid centres and the Worldwide LHC Computing Grid (WLCG) collaboration. The ALICE Collaboration acknowledges the following funding agencies for their support in building and running the ALICE detector: A. I. Alikhanyan National Science Laboratory (Yerevan Physics Institute) Foundation (ANSL), State Committee of Science and World Federation of Scientists (WFS), Armenia; Austrian Academy of Sciences, Austrian Science Fund (FWF): [M 2467-N36] and Nationalstiftung für Forschung, Technologie und Entwicklung, Austria; Ministry of Communications and High Technologies, National Nuclear Research Center, Azerbaijan; Conselho Nacional de Desenvolvimento Científico e Tecnológico (CNPq), Financiadora de Estudos e Projetos (Finep), Fundação de Amparo à Pesquisa do Estado de São Paulo (FAPESP) and Universidade Federal do Rio Grande do Sul (UFRGS), Brazil; Ministry of Education of China (MOEC), Ministry of Science & Technology of China (MSTC) and National Natural Science Foundation of China (NSFC), China; Ministry of Science and Education and Croatian Science Foundation, Croatia; Centro de Aplicaciones Tecnológicas y Desarrollo Nuclear (CEADEN), Cubaenergía, Cuba; Ministry of Education, Youth and Sports of the Czech Republic, Czech Republic; The Danish Council for Independent Research | Natural Sciences, the Villum Fonden and Danish National Research Foundation (DNRF), Denmark; Helsinki Institute of Physics (HIP), Finland; Commissariat à l'Energie Atomique (CEA) and Institut National de Physique Nucléaire et de Physique des Particules (IN2P3) and Centre National de la Recherche Scientifique (CNRS), France; Bundesministerium für Bildung und Forschung (BMBF) and GSI Helmholtzzentrum für Schwerionenforschung GmbH, Germany; General Secretariat for Research and Technology, Ministry of Education, Research and Religions, Greece; National Research, Development and Innovation Office, Hungary; Department of Atomic Energy Government of India (DAE), Department of Science and Technology, Government of India (DST), University Grants Commission, Government of India (UGC) and Council of Scientific and Industrial Research (CSIR), India; National Research and Innovation Agency - BRIN, Indonesia; Istituto Nazionale di Fisica Nucleare (INFN), Italy; Japanese Ministry of Education, Culture, Sports, Science and Technology (MEXT) and Japan Society for the Promotion of Science (JSPS) KAKENHI, Japan; Consejo Nacional de Ciencia (CONACYT) y Tecnología, through Fondo de Cooperación Internacional en Cien-

cia y Tecnología (FONCICYT) and Dirección General de Asuntos del Personal Académico (DGAPA), Mexico; Nederlandse Organisatie voor Wetenschappelijk Onderzoek (NWO), Netherlands; The Research Council of Norway, Norway; Commission on Science and Technology for Sustainable Development in the South (COMSATS), Pakistan; Pontificia Universidad Católica del Perú, Peru; Ministry of Education and Science, National Science Centre and WUT ID-UB, Poland; Korea Institute of Science and Technology Information and National Research Foundation of Korea (NRF), Republic of Korea; Ministry of Education and Scientific Research, Institute of Atomic Physics, Ministry of Research and Innovation and Institute of Atomic Physics and University Politehnica of Bucharest, Romania; Ministry of Education, Science, Research and Sport of the Slovak Republic, Slovakia; National Research Foundation of South Africa, South Africa; Swedish Research Council (VR) and Knut & Alice Wallenberg Foundation (KAW), Sweden; European Organization for Nuclear Research, Switzerland; Suranaree University of Technology (SUT), National Science and Technology Development Agency (NSTDA), Thailand Science Research and Innovation (TSRI) and National Science, Research and Innovation Fund (NSRF), Thailand; Turkish Energy, Nuclear and Mineral Research Agency (TEN-MAK), Turkey; National Academy of Sciences of Ukraine, Ukraine; Science and Technology Facilities Council (STFC), United Kingdom; National Science Foundation of the United States of America (NSF) and United States Department of Energy, Office of Nuclear Physics (DOE NP), United States of America. In addition, individual groups or members have received support from: Marie Skłodowska Curie, Strong 2020 - Horizon 2020 (grant nos. 824093, 896850), European Union; Academy of Finland (Center of Excellence in Quark Matter) (grant nos. 346327, 346328), Finland.

References

- [1] BRAHMS Collaboration, I.C. Arsene, et al., Nuclear stopping and rapidity loss in Au+Au collisions at $\sqrt{s_{NN}} = 62.4$ GeV, Phys. Lett. B 677 (2009) 267–271, arXiv: 0901.0872 [nucl-ex].
- [2] ALICE Collaboration, J. Adam, et al., Centrality dependence of the pseudorapidity density distribution for charged particles in Pb-Pb collisions at $\sqrt{s_{NN}} = 5.02$ TeV, Phys. Lett. B 772 (2017) 567–577, arXiv: 1612.08966 [nucl-ex].
- [3] NA50 Collaboration, M.C. Abreu, et al., Scaling of charged particle multiplicity in Pb-Pb collisions at SPS energies, Phys. Lett. B 530 (2002) 43–55.
- [4] PHOBOS Collaboration, B. Alver, et al., Charged-particle multiplicity and pseudorapidity distributions measured with the PHOBOS detector in Au+Au, Cu+Cu, d+Au, p+p collisions at ultrarelativistic energies, Phys. Rev. C 83 (2011) 024913, arXiv: 1011.1940 [nucl-ex].
- [5] ATLAS Collaboration, G. Aad, et al., Measurement of the centrality dependence of the charged-particle pseudorapidity distribution in proton-lead collisions at $\sqrt{s_{NN}} = 5.02$ TeV with the ATLAS detector, Eur. Phys. J. C 76 (2016) 199, arXiv: 1508.00848 [hep-ex].
- [6] BRAHMS Collaboration, I. Arsene, et al., Quark gluon plasma and color glass condensate at RHIC? The perspective from the BRAHMS experiment, Nucl. Phys. A 757 (2005) 1–27, arXiv: nucl-ex/0410020 [nucl-ex].
- [7] PHOBOS Collaboration, B.B. Back, et al., The PHOBOS perspective on discoveries at RHIC, Nucl. Phys. A 757 (2005) 28–101, arXiv: nucl-ex/0410022 [nucl-ex].
- [8] STAR Collaboration, J. Adams, et al., Experimental and theoretical challenges in the search for the quark gluon plasma: the STAR Collaboration's critical assessment of the evidence from RHIC collisions, Nucl. Phys. A 757 (2005) 102–183, arXiv: nucl-ex/0501009 [nucl-ex].
- [9] PHENIX Collaboration, K. Adcox, et al., Formation of dense partonic matter in relativistic nucleus-nucleus collisions at RHIC: experimental evaluation by the PHENIX collaboration, Nucl. Phys. A 757 (2005) 184–283, arXiv: nucl-ex/ 0410003 [nucl-ex].
- [10] C. Bierlich, T. Sjöstrand, M. Utneim, Hadronic rescattering in pA and AA collisions, Eur. Phys. J. A 57 (2021) 227, arXiv: 2103.09665 [hep-ph].
- [11] Z.-W. Lin, L. Zheng, Further developments of a multi-phase transport model for relativistic nuclear collisions, Nucl. Sci. Tech. 32 (2021) 113, arXiv: 2110.02989 [nucl-th].
- [12] J.D. Bjorken, Highly relativistic nucleus-nucleus collisions: the central rapidity region, Phys. Rev. D 27 (Jan 1983) 140–151.
- [13] H.-T. Ding, Recent lattice QCD results and phase diagram of strongly interacting matter, Nucl. Phys. A 931 (2014) 52–62, arXiv: 1408.5236 [hep-lat].
- [14] ALICE Collaboration, K. Aamodt, et al., The ALICE experiment at the CERN LHC, J. Instrum. 3 (2008) S08002.
- [15] ALICE Collaboration, B. Abelev, et al., Performance of the ALICE experiment at the CERN LHC, Int. J. Mod. Phys. A 29 (2014) 1430044, arXiv: 1402.4476 [nucl-ex].
- [16] ALICE Collaboration, J. Adam, et al., Charged-particle multiplicities in proton-proton collisions at $\sqrt{s} = 0.9$ to 8 TeV, Eur. Phys. J. C 77 (2017) 33, arXiv: 1509.07541 [nucl-ex].
- [17] ALICE Collaboration, S. Acharya, et al., Pseudorapidity distributions of charged particles as a function of mid- and forward rapidity multiplicities in pp collisions at $\sqrt{s} = 5.02, 7$ and 13 TeV, Eur. Phys. J. C 81 (2021) 630, arXiv: 2009.09434 [nucl-ex].
- [18] ALICE Collaboration, K. Aamodt, et al., Charged-particle multiplicity density at mid-rapidity in central Pb-Pb collisions at $\sqrt{s_{NN}} = 2.76$ TeV, Phys. Rev. Lett. 105 (2010) 252301, arXiv: 1011.3916 [nucl-ex].
- [19] ALICE Collaboration, B. Abelev, et al., Centrality determination of Pb-Pb collisions at $\sqrt{s_{NN}} = 2.76$ TeV with ALICE, Phys. Rev. C 88 (2013) 044909, arXiv: 1301.4361 [nucl-ex].
- [20] ALICE Collaboration, J. Adam, et al., Centrality dependence of particle production in p-Pb collisions at $\sqrt{s_{NN}} = 5.02$ TeV, Phys. Rev. C 91 (2015) 064905, arXiv: 1412.6828 [nucl-ex].
- [21] ALICE Collaboration, S. Acharya, et al., The ALICE definition of primary particles, ALICE-PUBLIC-2017-005, <https://cds.cern.ch/record/2270008>.
- [22] ALICE Collaboration, J. Adam, et al., Centrality evolution of the charged-particle pseudorapidity density over a broad pseudorapidity range in Pb-Pb collisions at $\sqrt{s_{NN}} = 2.76$ TeV, Phys. Lett. B 754 (2016) 373–385, arXiv: 1509.07299 [nucl-ex].
- [23] ALICE Collaboration, J. Adam, et al., Centrality dependence of the charged-particle multiplicity density at midrapidity in Pb-Pb collisions at $\sqrt{s_{NN}} = 5.02$ TeV, Phys. Rev. Lett. 116 (2016) 222302, arXiv: 1512.06104 [nucl-ex].
- [24] ALICE Collaboration, S. Acharya, et al., Charged-particle production as a function of multiplicity and transverse sphericity in pp collisions at $\sqrt{s} = 5.02$ and 13 TeV, Eur. Phys. J. C 79 (2019) 857, arXiv: 1905.07208 [nucl-ex].
- [25] S.J. Brodsky, et al., Hadron production in nuclear collisions: a new parton model approach, Phys. Rev. Lett. 39 (1977) 1120.
- [26] A. Adil, et al., 3D jet tomography of twisted strongly coupled quark gluon plasmas, Phys. Rev. C 72 (2005) 034907, arXiv: nucl-th/0505004 [nucl-th].
- [27] ALICE Collaboration, E. Abbas, et al., Centrality dependence of the pseudorapidity density distribution for charged particles in Pb-Pb collisions at $\sqrt{s_{NN}} = 2.76$ TeV, Phys. Lett. B 726 (2013) 610–622, arXiv: 1304.0347 [nucl-ex].
- [28] ALICE Collaboration, S. Acharya, et al., Centrality determination in heavy ion collisions, ALICE-PUBLIC-2018-011, <http://cds.cern.ch/record/2636623>.
- [29] T. Pierog, et al., EPOS LHC: test of collective hadronization with data measured at the CERN Large Hadron Collider, Phys. Rev. C 92 (2015) 034906, arXiv: 1306.0121 [hep-ph].
- [30] ALICE Collaboration, B. Abelev, et al., Centrality dependence of π , K, p production in Pb-Pb collisions at $\sqrt{s_{NN}} = 2.76$ TeV, Phys. Rev. C 88 (2013) 044910, arXiv: 1303.0737 [hep-ex].
- [31] ALICE Collaboration, J. Adam, et al., Measurement of transverse energy at midrapidity in Pb-Pb collisions at $\sqrt{s_{NN}} = 2.76$ TeV, Phys. Rev. C 94 (2016) 034903, arXiv: 1603.04775 [nucl-ex].
- [32] C. Loizides, J. Nagle, P. Steinberg, Improved version of the PHOBOS Glauber Monte Carlo, SoftwareX 1–2 (2015) 13–18.
- [33] C. Loizides, Glauber modeling of high-energy nuclear collisions at the subnucleon level, Phys. Rev. C 94 (2016) 024914, arXiv: 1603.07375 [nucl-ex].

ALICE Collaboration

S. Acharya ^{123, 130,} , D. Adamová ^{85,} , A. Adler ⁶⁸, G. Aglieri Rinella ^{32,} , M. Agnello ^{29,} , N. Agrawal ^{49,} , Z. Ahammed ^{130,} , S. Ahmad ^{15,} , S.U. Ahn ^{69,} , I. Ahuja ^{36,} , A. Akindinov ^{138,} , M. Al-Turany ^{97,} , D. Aleksandrov ^{138,} , B. Alessandro ^{54,} , H.M. Alfanda ^{6,} , R. Alfaro Molina ^{65,} , B. Ali ^{15,} , Y. Ali ^{13,} , A. Alici ^{25,} , N. Alizadehvandchali ^{112,} , A. Alkin ^{32,} , J. Alme ^{20,} , G. Alocco ^{50,} , T. Alt ^{62,} , I. Altsybeev ^{138,} , M.N. Anaam ^{6,} , C. Andrei ^{44,} , A. Andronic ^{133,} , V. Anguelov ^{94,} ,

- F. Antinori ^{52, ID}, P. Antonioli ^{49, ID}, C. Anuj ^{15, ID}, N. Apadula ^{73, ID}, L. Aphecetche ^{102, ID},
 H. Appelshäuser ^{62, ID}, S. Arcelli ^{25, ID}, R. Arnaldi ^{54, ID}, I.C. Arsene ^{19, ID}, M. Arslanbekov ^{135, ID},
 A. Augustinus ^{32, ID}, R. Averbeck ^{97, ID}, S. Aziz ^{71, ID}, M.D. Azmi ^{15, ID}, A. Badalà ^{51, ID}, Y.W. Baek ^{39, ID},
 X. Bai ^{97, ID}, R. Bailhache ^{62, ID}, Y. Bailung ^{46, ID}, R. Bala ^{90, ID}, A. Balbino ^{29, ID}, A. Baldissari ^{126, ID},
 B. Balis ^{2, ID}, D. Banerjee ^{4, ID}, Z. Banoo ^{90, ID}, R. Barbera ^{26, ID}, L. Barioglio ^{95, ID}, M. Barlou ⁷⁷,
 G.G. Barnaföldi ^{134, ID}, L.S. Barnby ^{84, ID}, V. Barret ^{123, ID}, L. Barreto ^{108, ID}, C. Bartels ^{115, ID}, K. Barth ^{32, ID},
 E. Bartsch ^{62, ID}, F. Baruffaldi ^{27, ID}, N. Bastid ^{123, ID}, S. Basu ^{74, ID}, G. Batigne ^{102, ID}, D. Battistini ^{95, ID},
 B. Batyunya ^{139, ID}, D. Bauri ⁴⁵, J.L. Bazo Alba ^{100, ID}, I.G. Bearden ^{82, ID}, C. Beattie ^{135, ID}, P. Becht ^{97, ID},
 I. Belikov ^{125, ID}, A.D.C. Bell Hechavarria ^{133, ID}, R. Bellwied ^{112, ID}, S. Belokurova ^{138, ID}, V. Belyaev ^{138, ID},
 G. Bencedi ^{134, 63, ID}, S. Beole ^{24, ID}, A. Bercuci ^{44, ID}, Y. Berdnikov ^{138, ID}, A. Berdnikova ^{94, ID},
 L. Bergmann ^{94, ID}, M.G. Besoiu ^{61, ID}, L. Betev ^{32, ID}, P.P. Bhaduri ^{130, ID}, A. Bhasin ^{90, ID}, I.R. Bhat ⁹⁰,
 M.A. Bhat ^{4, ID}, B. Bhattacharjee ^{40, ID}, L. Bianchi ^{24, ID}, N. Bianchi ^{47, ID}, J. Bielčík ^{35, ID}, J. Bielčíková ^{85, ID},
 J. Biernat ^{105, ID}, A. Bilandzic ^{95, ID}, G. Biro ^{134, ID}, S. Biswas ^{4, ID}, J.T. Blair ^{106, ID}, D. Blau ^{138, ID},
 M.B. Blidaru ^{97, ID}, N. Bluhme ³⁷, C. Blume ^{62, ID}, G. Boca ^{21, 53, ID}, F. Bock ^{86, ID}, A. Bogdanov ¹³⁸, S. Boi ^{22, ID},
 J. Bok ^{56, ID}, L. Boldizsár ^{134, ID}, A. Bolozdynya ^{138, ID}, M. Bombara ^{36, ID}, P.M. Bond ^{32, ID}, G. Bonomi ^{129, 53, ID},
 H. Borel ^{126, ID}, A. Borissov ^{138, ID}, H. Bossi ^{135, ID}, E. Botta ^{24, ID}, L. Bratrud ^{62, ID}, P. Braun-Munzinger ^{97, ID},
 M. Bregant ^{108, ID}, M. Broz ^{35, ID}, G.E. Bruno ^{96, 31, ID}, M.D. Buckland ^{115, ID}, D. Budnikov ^{138, ID},
 H. Buesching ^{62, ID}, S. Bufalino ^{29, ID}, O. Bugnon ¹⁰², P. Buhler ^{101, ID}, Z. Buthelezi ^{66, 119, ID}, J.B. Butt ¹³,
 A. Bylinkin ^{114, ID}, S.A. Bysiak ¹⁰⁵, M. Cai ^{27, 6, ID}, H. Caines ^{135, ID}, A. Caliva ^{97, ID}, E. Calvo Villar ^{100, ID},
 J.M.M. Camacho ^{107, ID}, R.S. Camacho ⁴³, P. Camerini ^{23, ID}, F.D.M. Canedo ^{108, ID}, M. Carabas ^{122, ID},
 F. Carnesecchi ^{25, ID}, R. Caron ^{124, 126, ID}, J. Castillo Castellanos ^{126, ID}, F. Catalano ^{29, ID}, C. Ceballos
 Sanchez ^{139, ID}, I. Chakaberia ^{73, ID}, P. Chakraborty ^{45, ID}, S. Chandra ^{130, ID}, S. Chapelard ^{32, ID},
 M. Chartier ^{115, ID}, S. Chattopadhyay ^{130, ID}, S. Chattopadhyay ^{98, ID}, T.G. Chavez ^{43, ID}, T. Cheng ^{6, ID},
 C. Cheshkov ^{124, ID}, B. Cheynis ^{124, ID}, V. Chibante Barroso ^{32, ID}, D.D. Chinellato ^{109, ID}, E.S. Chizzali ^{95, ID, II},
 S. Cho ^{56, ID}, P. Chochula ^{32, ID}, P. Christakoglou ^{83, ID}, C.H. Christensen ^{82, ID}, P. Christiansen ^{74, ID},
 T. Chujo ^{121, ID}, M. Ciacco ^{29, ID}, C. Ciccolo ^{50, ID}, L. Cifarelli ^{25, ID}, F. Cindolo ^{49, ID}, M.R. Ciupak ⁹⁷, G. Clai ^{49, III},
 J. Cleymans ^{111, I}, F. Colamaria ^{48, ID}, J.S. Colburn ⁹⁹, D. Colella ^{48, ID}, A. Collu ⁷³, M. Colocci ^{32, ID},
 M. Concas ^{54, ID, IV}, G. Conesa Balbastre ^{72, ID}, Z. Conesa del Valle ^{71, ID}, G. Contin ^{23, ID}, J.G. Contreras ^{35, ID},
 M.L. Coquet ^{126, ID}, T.M. Cormier ^{86, I}, P. Cortese ^{128, ID}, M.R. Cosentino ^{110, ID}, F. Costa ^{32, ID},
 S. Costanza ^{21, 53, ID}, P. Crochet ^{123, ID}, R. Cruz-Torres ^{73, ID}, E. Cuautle ⁶³, P. Cui ^{6, ID}, L. Cunqueiro ⁸⁶,
 A. Dainese ^{52, ID}, M.C. Danisch ^{94, ID}, A. Danu ^{61, ID}, P. Das ^{79, ID}, P. Das ^{4, ID}, S. Das ^{4, ID}, S. Dash ^{45, ID},
 R.M.H. David ⁴³, A. De Caro ^{28, ID}, G. de Cataldo ^{48, ID}, L. De Cilladi ^{24, ID}, J. de Cuveland ³⁷, A. De Falco ^{22, ID},
 D. De Gruttola ^{28, ID}, N. De Marco ^{54, ID}, C. De Martin ^{23, ID}, S. De Pasquale ^{28, ID}, S. Deb ^{46, ID},
 H.F. Degenhardt ¹⁰⁸, K.R. Deja ¹³¹, R. Del Grande ^{95, ID}, L. Dello Stritto ^{28, ID}, W. Deng ^{6, ID}, P. Dhankher ^{18, ID},
 D. Di Bari ^{31, ID}, A. Di Mauro ^{32, ID}, R.A. Diaz ^{139, 7, ID}, T. Dietel ^{111, ID}, Y. Ding ^{124, 6, ID}, R. Divià ^{32, ID},
 D.U. Dixit ^{18, ID}, Ø. Djupsland ²⁰, U. Dmitrieva ^{138, ID}, A. Dobrin ^{61, ID}, B. Dönigus ^{62, ID}, A.K. Dubey ^{130, ID},
 J.M. Dubinski ^{131, ID}, A. Dubla ^{97, 83, ID}, S. Dudi ^{89, ID}, P. Dupieux ^{123, ID}, M. Durkac ¹⁰⁴, N. Dzalaiova ¹²,
 T.M. Eder ^{133, ID}, R.J. Ehlers ^{86, ID}, V.N. Eikeland ²⁰, F. Eisenhut ^{62, ID}, D. Elia ^{48, ID}, B. Erazmus ^{102, ID},
 F. Ercolelli ^{25, ID}, F. Erhardt ^{88, ID}, A. Erokhin ¹³⁸, M.R. Ersdal ²⁰, B. Espagnon ^{71, ID}, G. Eulisse ^{32, ID},
 D. Evans ^{99, ID}, S. Evdokimov ^{138, ID}, L. Fabbietti ^{95, ID}, M. Faggin ^{27, ID}, J. Faivre ^{72, ID}, F. Fan ^{6, ID}, W. Fan ^{73, ID},
 A. Fantoni ^{47, ID}, M. Fasel ^{86, ID}, P. Fecchio ²⁹, A. Feliciello ^{54, ID}, G. Feofilov ^{138, ID}, A. Fernández Téllez ^{43, ID},
 A. Ferrero ^{126, ID}, A. Ferretti ^{24, ID}, V.J.G. Feuillard ^{94, ID}, J. Figiel ^{105, ID}, V. Filova ^{35, ID}, D. Finogeev ^{138, ID},

- G. Fiorenza 96, F. Flor 112, ID, A.N. Flores 106, ID, S. Foertsch 66, ID, I. Fokin 94, ID, S. Fokin 138, ID,
 E. Fragiocomo 55, ID, E. Frajna 134, ID, U. Fuchs 32, ID, N. Funicello 28, ID, C. Furget 72, ID, A. Furs 138, ID,
 J.J. Gaardhøje 82, ID, M. Gagliardi 24, ID, A.M. Gago 100, ID, A. Gal 125, C.D. Galvan 107, ID, P. Ganoti 77, ID,
 C. Garabatos 97, ID, J.R.A. Garcia 43, ID, E. Garcia-Solis 9, ID, K. Garg 102, ID, C. Gargiulo 32, ID, A. Garibli 80,
 K. Garner 133, E.F. Gauger 106, ID, A. Gautam 114, ID, M.B. Gay Ducati 64, ID, M. Germain 102, ID, S.K. Ghosh 4,
 M. Giacalone 25, ID, P. Gianotti 47, ID, P. Giubellino 97, 54, ID, P. Giubilato 27, ID, A.M.C. Glaenzer 126, ID,
 P. Glässel 94, ID, E. Glimos 118, ID, D.J.Q. Goh 75, V. Gonzalez 132, ID, L.H. González-Trueba 65, ID,
 S. Gorbunov 37, M. Gorgon 2, ID, L. Görlich 105, ID, S. Gotovac 33, V. Grabski 65, ID, L.K. Graczykowski 131, ID,
 E. Grecka 85, ID, L. Greiner 73, ID, A. Grelli 57, ID, C. Grigoras 32, ID, V. Grigoriev 138, ID, S. Grigoryan 139, 1, ID,
 F. Grossa 54, ID, J.F. Grosse-Oetringhaus 32, ID, R. Grossi 97, ID, D. Grund 35, ID, G.G. Guardiano 109, ID,
 R. Guernane 72, ID, M. Guilbaud 102, ID, K. Gulbrandsen 82, ID, T. Gunji 120, ID, W. Guo 6, ID, A. Gupta 90, ID,
 R. Gupta 90, ID, S.P. Guzman 43, ID, L. Gyulai 134, ID, M.K. Habib 97, C. Hadjidakis 71, ID, H. Hamagaki 75, ID,
 M. Hamid 6, R. Hannigan 106, ID, M.R. Haque 131, ID, A. Harlenderova 97, J.W. Harris 135, ID, A. Harton 9, ID,
 J.A. Hasenbichler 32, H. Hassan 86, ID, D. Hatzifotiadou 49, ID, P. Hauer 41, ID, L.B. Havener 135, ID,
 S.T. Heckel 95, ID, E. Hellbär 97, ID, H. Helstrup 34, ID, T. Herman 35, ID, G. Herrera Corral 8, ID, F. Herrmann 133,
 K.F. Hetland 34, ID, B. Heybeck 62, ID, H. Hillemanns 32, ID, C. Hills 115, ID, B. Hippolyte 125, ID, B. Hofman 57, ID,
 B. Hohlweger 83, ID, J. Honermann 133, ID, G.H. Hong 136, ID, D. Horak 35, ID, A. Horzyk 2, ID, R. Hosokawa 14,
 Y. Hou 6, ID, P. Hristov 32, ID, C. Hughes 118, ID, P. Huhn 62, L.M. Huhta 113, ID, C.V. Hulse 71, ID,
 T.J. Humanic 87, ID, H. Hushnud 98, A. Hutson 112, ID, D. Hutter 37, ID, J.P. Iddon 115, ID, R. Ilkaev 138,
 H. Ilyas 13, ID, M. Inaba 121, ID, G.M. Innocenti 32, ID, M. Ippolitov 138, ID, A. Isakov 85, ID, T. Isidori 114, ID,
 M.S. Islam 98, ID, M. Ivanov 97, ID, V. Ivanov 138, ID, V. Izucheev 138, M. Jablonski 2, ID, B. Jacak 73, ID,
 N. Jacazio 32, ID, P.M. Jacobs 73, ID, S. Jadlovska 104, J. Jadlovsky 104, C. Jahnke 109, ID, A. Jalotra 90,
 M.A. Janik 131, ID, T. Janson 68, M. Jercic 88, O. Jevons 99, A.A.P. Jimenez 63, ID, F. Jonas 86, 133, ID, P.G. Jones 99,
 J.M. Jowett 32, 97, ID, J. Jung 62, ID, M. Jung 62, ID, A. Junique 32, ID, A. Jusko 99, ID, M.J. Kabus 131, ID,
 J. Kaewjai 103, P. Kalinak 58, ID, A.S. Kalteyer 97, ID, A. Kalweit 32, ID, V. Kaplin 138, ID, A. Karasu Uysal 70, ID,
 D. Karatovic 88, ID, O. Karavichev 138, ID, T. Karavicheva 138, ID, P. Karczmarczyk 131, ID, E. Karpechev 138, ID,
 V. Kashyap 79, A. Kazantsev 138, U. Kebschull 68, ID, R. Keidel 137, ID, D.L.D. Keijdener 57, M. Keil 32, ID,
 B. Ketzer 41, ID, A.M. Khan 6, ID, S. Khan 15, ID, A. Khanzadeev 138, ID, Y. Kharlov 138, ID, A. Khatun 15, ID,
 A. Khuntia 105, ID, B. Kileng 34, ID, B. Kim 16, ID, C. Kim 16, ID, D.J. Kim 113, ID, E.J. Kim 67, ID, J. Kim 136, ID,
 J.S. Kim 39, ID, J. Kim 94, ID, J. Kim 67, ID, M. Kim 94, ID, S. Kim 17, ID, T. Kim 136, ID, S. Kirsch 62, ID, I. Kisel 37, ID,
 S. Kiselev 138, ID, A. Kisiel 131, ID, J.P. Kitowski 2, ID, J.L. Klay 5, ID, J. Klein 32, ID, S. Klein 73, ID,
 C. Klein-Bösing 133, ID, M. Kleiner 62, ID, T. Klemenz 95, ID, A. Kluge 32, ID, A.G. Knospe 112, ID, C. Kobdaj 103, ID,
 T. Kollegger 97, A. Kondratyev 139, ID, N. Kondratyeva 138, ID, E. Kondratyuk 138, ID, J. Konig 62, ID,
 S.A. Konigstorfer 95, ID, P.J. Konopka 32, ID, G. Kornakov 131, ID, S.D. Koryciak 2, ID, A. Kotliarov 85, ID,
 O. Kovalenko 78, ID, V. Kovalenko 138, ID, M. Kowalski 105, ID, I. Králik 58, ID, A. Kravčáková 36, ID, L. Kreis 97,
 M. Krivda 99, 58, ID, F. Krizek 85, ID, K. Krizkova Gajdosova 35, ID, M. Kroesen 94, ID, M. Krüger 62, ID,
 D.M. Krupova 35, ID, E. Kryshen 138, ID, M. Krzewicki 37, V. Kučera 32, ID, C. Kuhn 125, ID, P.G. Kuijer 83, ID,
 T. Kumaoka 121, D. Kumar 130, L. Kumar 89, ID, N. Kumar 89, S. Kundu 32, ID, P. Kurashvili 78, ID,
 A. Kurepin 138, ID, A.B. Kurepin 138, ID, A. Kuryakin 138, ID, S. Kushpil 85, ID, J. Kvapil 99, ID, M.J. Kweon 56, ID,
 J.Y. Kwon 56, ID, Y. Kwon 136, ID, S.L. La Pointe 37, ID, P. La Rocca 26, ID, Y.S. Lai 73, A. Lakrathok 103,
 M. Lamanna 32, ID, R. Langoy 117, ID, P. Larionov 47, ID, E. Laudi 32, ID, L. Lautner 32, 95, ID, R. Lavicka 101, 35, ID,
 T. Lazareva 138, ID, R. Lea 129, 53, ID, J. Lehrbach 37, ID, R.C. Lemmon 84, ID, I. León Monzón 107, ID,

- M.M. Lesch 95, ID, E.D. Lesser 18, ID, M. Lettrich 32, 95, P. Léval 134, ID, X. Li 10, X.L. Li 6, J. Lien 117, ID,
 R. Lietava 99, ID, B. Lim 16, ID, S.H. Lim 16, ID, V. Lindenstruth 37, ID, A. Lindner 44, C. Lippmann 97, ID,
 A. Liu 18, ID, D.H. Liu 6, ID, J. Liu 115, ID, I.M. Lofnes 20, ID, V. Loginov 138, C. Loizides 86, ID, P. Loncar 33, ID,
 J.A. Lopez 94, ID, X. Lopez 123, ID, E. López Torres 7, ID, P. Lu 116, ID, J.R. Luhder 133, ID, M. Lunardon 27, ID,
 G. Luparello 55, ID, Y.G. Ma 38, ID, A. Maevskaya 138, M. Mager 32, ID, T. Mahmoud 41, A. Maire 125, ID,
 M. Malaev 138, ID, N.M. Malik 90, ID, Q.W. Malik 19, S.K. Malik 90, ID, L. Malinina 139, ID, VII
 D. Mal'Kovich 138, ID, D. Mallick 79, ID, N. Mallick 46, ID, G. Mandaglio 30, 51, ID, V. Manko 138, ID,
 F. Manso 123, ID, V. Manzari 48, ID, Y. Mao 6, ID, G.V. Margagliotti 23, ID, A. Margotti 49, ID, A. Marín 97, ID,
 C. Markert 106, ID, M. Marquard 62, N.A. Martin 94, P. Martinengo 32, ID, J.L. Martinez 112, M.I. Martínez 43, ID,
 G. Martínez García 102, ID, S. Masciocchi 97, ID, M. Masera 24, ID, A. Masoni 50, ID, L. Massacrier 71, ID,
 A. Mastroserio 127, 48, ID, A.M. Mathis 95, ID, O. Matonoha 74, ID, P.F.T. Matuoka 108, A. Matyja 105, ID,
 C. Mayer 105, ID, A.L. Mazuecos 32, ID, F. Mazzaschi 24, ID, M. Mazzilli 32, ID, J.E. Mdhluli 119, ID, A.F. Mechler 62,
 Y. Melikyan 138, ID, A. Menchaca-Rocha 65, ID, E. Meninno 101, 28, ID, A.S. Menon 112, ID, M. Meres 12, ID,
 S. Mhlanga 111, 66, Y. Miake 121, L. Micheletti 54, ID, L.C. Migliorin 124, D.L. Mihaylov 95, ID,
 K. Mikhaylov 139, 138, ID, A.N. Mishra 134, ID, D. Miśkowiec 97, ID, A. Modak 4, ID, A.P. Mohanty 57, ID,
 B. Mohanty 79, M. Mohisin Khan 15, ID, V, M.A. Molander 42, ID, Z. Moravcova 82, ID, C. Mordasini 95, ID,
 D.A. Moreira De Godoy 133, ID, I. Morozov 138, ID, A. Morsch 32, ID, T. Mrnjavac 32, ID, V. Muccifora 47, ID,
 E. Mudnic 33, S. Muhuri 130, ID, J.D. Mulligan 73, ID, A. Mulliri 22, M.G. Munhoz 108, ID, R.H. Munzer 62, ID,
 H. Murakami 120, ID, S. Murray 111, ID, L. Musa 32, ID, J. Musinsky 58, ID, J.W. Myrcha 131, ID, B. Naik 119, ID,
 R. Nair 78, ID, B.K. Nandi 45, ID, R. Nania 49, ID, E. Nappi 48, ID, A.F. Nassirpour 74, ID, A. Nath 94, ID,
 C. Nattrass 118, ID, A. Neagu 19, A. Negru 122, L. Nellen 63, ID, S.V. Nesbo 34, G. Neskovic 37, ID,
 D. Nesterov 138, ID, B.S. Nielsen 82, ID, E.G. Nielsen 82, ID, S. Nikolaev 138, ID, S. Nikulin 138, ID, V. Nikulin 138, ID,
 F. Noferini 49, ID, S. Noh 11, ID, P. Nomokonov 139, ID, J. Norman 115, ID, N. Novitzky 121, ID,
 P. Nowakowski 131, ID, A. Nyanin 138, ID, J. Nystrand 20, ID, M. Ogino 75, ID, A. Ohlson 74, ID,
 V.A. Okorokov 138, ID, J. Oleniacz 131, ID, A.C. Oliveira Da Silva 118, ID, M.H. Oliver 135, ID, A. Onnerstad 113, ID,
 C. Oppedisano 54, ID, A. Ortiz Velasquez 63, ID, A. Oskarsson 74, J. Otwinowski 105, ID, M. Oya 92,
 K. Oyama 75, ID, Y. Pachmayer 94, ID, S. Padhan 45, ID, D. Pagano 129, 53, ID, G. Paić 63, ID, A. Palasciano 48, ID,
 S. Panebianco 126, ID, J. Park 56, ID, J.E. Parkkila 32, 113, ID, S.P. Pathak 112, R.N. Patra 32, B. Paul 22, ID,
 H. Pei 6, ID, T. Peitzmann 57, ID, X. Peng 6, ID, L.G. Pereira 64, ID, H. Pereira Da Costa 126, ID, D. Peresunko 138, ID,
 G.M. Perez 7, ID, S. Perrin 126, ID, Y. Pestov 138, V. Petráček 35, ID, V. Petrov 138, ID, M. Petrovici 44, ID,
 R.P. Pezzi 64, ID, S. Piano 55, ID, M. Pikna 12, ID, P. Pillot 102, ID, O. Pinazza 49, 32, ID, L. Pinsky 112,
 C. Pinto 95, 26, ID, S. Pisano 47, ID, M. Płoskoń 73, ID, M. Planinic 88, F. Pliquet 62, M.G. Poghosyan 86, ID,
 B. Polichtchouk 138, ID, S. Politano 29, ID, N. Poljak 88, ID, A. Pop 44, ID, S. Porteboeuf-Houssais 123, ID,
 J. Porter 73, ID, V. Pozdniakov 139, ID, S.K. Prasad 4, ID, R. Preghenella 49, ID, F. Prino 54, ID, C.A. Pruneau 132, ID,
 I. Pshenichnov 138, ID, M. Puccio 32, ID, S. Qiu 83, ID, L. Quaglia 24, ID, R.E. Quishpe 112, S. Ragoni 99, ID,
 A. Rakotozafindrabe 126, ID, L. Ramello 128, ID, F. Rami 125, ID, S.A.R. Ramirez 43, ID, T.A. Rancien 72,
 R. Raniwala 91, ID, S. Raniwala 91, S.S. Räsänen 42, ID, R. Rath 46, ID, I. Ravasenga 83, ID, K.F. Read 86, 118, ID,
 A.R. Redelbach 37, ID, K. Redlich 78, ID, VI, A. Rehman 20, P. Reichelt 62, F. Reidt 32, ID, H.A. Reme-Ness 34, ID,
 Z. Rescakova 36, K. Reygers 94, ID, A. Riabov 138, ID, V. Riabov 138, ID, R. Ricci 28, ID, T. Richert 74,
 M. Richter 19, ID, W. Riegler 32, ID, F. Riggi 26, ID, C. Ristea 61, ID, M. Rodríguez Cahuantzi 43, ID, K. Røed 19, ID,
 R. Rogalev 138, ID, E. Rogochaya 139, ID, T.S. Rogoschinski 62, ID, D. Rohr 32, ID, D. Röhrich 20, ID, P.F. Rojas 43,
 S. Rojas Torres 35, ID, P.S. Rokita 131, ID, F. Ronchetti 47, ID, A. Rosano 30, 51, ID, E.D. Rosas 63, A. Rossi 52, ID,

- A. Roy ^{46, ID}, P. Roy ⁹⁸, S. Roy ^{45, ID}, N. Rubini ^{25, ID}, O.V. Rueda ^{74, ID}, D. Ruggiano ^{131, ID}, R. Rui ^{23, ID},
 B. Rumyantsev ¹³⁹, P.G. Russek ^{2, ID}, R. Russo ^{83, ID}, A. Rustamov ^{80, ID}, E. Ryabinkin ^{138, ID}, Y. Ryabov ^{138, ID},
 A. Rybicki ^{105, ID}, H. Rytkonen ^{113, ID}, W. Rzesz ^{131, ID}, O.A.M. Saarimaki ^{42, ID}, R. Sadek ^{102, ID},
 S. Sadovsky ^{138, ID}, J. Saetre ^{20, ID}, K. Šafařík ^{35, ID}, S.K. Saha ^{130, ID}, S. Saha ^{79, ID}, B. Sahoo ^{45, ID}, P. Sahoo ⁴⁵,
 R. Sahoo ^{46, ID}, S. Sahoo ⁵⁹, D. Sahu ^{46, ID}, P.K. Sahu ^{59, ID}, J. Saini ^{130, ID}, S. Sakai ^{121, ID}, M.P. Salvan ^{97, ID},
 S. Sambyal ^{90, ID}, T.B. Saramela ¹⁰⁸, D. Sarkar ^{132, ID}, N. Sarkar ¹³⁰, P. Sarma ^{40, ID}, V.M. Sarti ^{95, ID},
 M.H.P. Sas ^{135, ID}, J. Schambach ^{86, ID}, H.S. Scheid ^{62, ID}, C. Schiaua ^{44, ID}, R. Schicker ^{94, ID}, A. Schmah ⁹⁴,
 C. Schmidt ^{97, ID}, H.R. Schmidt ⁹³, M.O. Schmidt ^{32, ID}, M. Schmidt ⁹³, N.V. Schmidt ^{86, 62, ID},
 A.R. Schmier ^{118, ID}, R. Schotter ^{125, ID}, J. Schukraft ^{32, ID}, K. Schwarz ⁹⁷, K. Schweda ^{97, ID}, G. Scioli ^{25, ID},
 E. Scomparin ^{54, ID}, J.E. Seger ^{14, ID}, Y. Sekiguchi ¹²⁰, D. Sekihata ^{120, ID}, I. Selyuzhenkov ^{97, 138, ID},
 S. Senyukov ^{125, ID}, J.J. Seo ^{56, ID}, D. Serebryakov ^{138, ID}, L. Šerkšnytė ^{95, ID}, A. Sevcenco ^{61, ID}, T.J. Shaba ^{66, ID},
 A. Shabanov ¹³⁸, A. Shabetai ^{102, ID}, R. Shahoyan ³², W. Shaikh ⁹⁸, A. Shangaraev ^{138, ID}, A. Sharma ⁸⁹,
 D. Sharma ^{45, ID}, H. Sharma ^{105, ID}, M. Sharma ^{90, ID}, N. Sharma ^{89, ID}, S. Sharma ^{90, ID}, U. Sharma ^{90, ID},
 A. Shatat ^{71, ID}, O. Sheibani ¹¹², K. Shigaki ^{92, ID}, M. Shimomura ⁷⁶, S. Shirinkin ^{138, ID}, Q. Shou ^{38, ID},
 Y. Sibirjak ^{138, ID}, S. Siddhanta ^{50, ID}, T. Siemiarczuk ^{78, ID}, T.F. Silva ^{108, ID}, D. Silvermyr ^{74, ID},
 T. Simantathammakul ¹⁰³, G. Simonetti ³², B. Singh ^{95, ID}, R. Singh ^{79, ID}, R. Singh ^{90, ID}, R. Singh ^{46, ID},
 V.K. Singh ^{130, ID}, V. Singhal ^{130, ID}, T. Sinha ^{98, ID}, B. Sitar ^{12, ID}, M. Sitta ^{128, ID}, T.B. Skaali ¹⁹,
 G. Skorodumovs ^{94, ID}, M. Slupecki ^{42, ID}, N. Smirnov ^{135, ID}, R.J.M. Snellings ^{57, ID}, C. Soncco ¹⁰⁰,
 J. Song ^{112, ID}, A. Songmoolnak ¹⁰³, F. Soramel ^{27, ID}, S. Sorensen ^{118, ID}, I. Sputowska ^{105, ID}, J. Stachel ^{94, ID},
 I. Stan ^{61, ID}, P.J. Steffanic ^{118, ID}, S.F. Stiefelmaier ^{94, ID}, D. Stocco ^{102, ID}, I. Storehaug ^{19, ID},
 M.M. Storetvedt ^{34, ID}, P. Stratmann ^{133, ID}, S. Strazzi ^{25, ID}, C.P. Stylianidis ⁸³, A.A.P. Suaide ^{108, ID},
 C. Suire ^{71, ID}, M. Sukhanov ^{138, ID}, M. Suljic ^{32, ID}, R. Sultanov ^{138, ID}, V. Sumberia ^{90, ID},
 S. Sumowidagdo ^{81, ID}, S. Swain ⁵⁹, A. Szabo ¹², I. Szarka ^{12, ID}, U. Tabassam ¹³, S.F. Taghavi ^{95, ID},
 G. Taillepied ^{97, 123, ID}, J. Takahashi ^{109, ID}, G.J. Tambave ^{20, ID}, S. Tang ^{123, 6, ID}, Z. Tang ^{116, ID}, J.D. Tapia
 Takaki ^{114, ID}, N. Tapus ¹²², L.A. Tarasovicova ^{133, ID}, M.G. Tarzila ^{44, ID}, A. Tauro ^{32, ID}, G. Tejeda Muñoz ^{43, ID},
 A. Telesca ^{32, ID}, L. Terlizzi ^{24, ID}, C. Terrevoli ^{112, ID}, G. Tersimonov ³, S. Thakur ^{130, ID}, D. Thomas ^{106, ID},
 R. Tieulent ^{124, ID}, A. Tikhonov ^{138, ID}, A.R. Timmins ^{112, ID}, M. Tkacik ¹⁰⁴, T. Tkacik ^{104, ID}, A. Toia ^{62, ID},
 N. Topilskaya ^{138, ID}, M. Toppi ^{47, ID}, F. Torales-Acosta ¹⁸, T. Tork ^{71, ID}, A.G. Torres Ramos ^{31, ID},
 A. Trifiró ^{30, 51, ID}, A.S. Triolo ^{30, 51, ID}, S. Tripathy ^{49, ID}, T. Tripathy ^{45, ID}, S. Trogolo ^{32, ID}, V. Trubnikov ^{3, ID},
 W.H. Trzaska ^{113, ID}, T.P. Trzcinski ^{131, ID}, A. Tumkin ^{138, ID}, R. Turrisi ^{52, ID}, T.S. Tveter ^{19, ID}, K. Ullaland ^{20, ID},
 A. Uras ^{124, ID}, M. Urioni ^{53, 129, ID}, G.L. Usai ^{22, ID}, M. Vala ³⁶, N. Valle ^{21, ID}, S. Vallero ^{54, ID}, L.V.R. van
 Doremalen ⁵⁷, M. van Leeuwen ^{83, ID}, R.J.G. van Weelden ^{83, ID}, P. Vande Vyvre ^{32, ID}, D. Varga ^{134, ID},
 Z. Varga ^{134, ID}, M. Varga-Kofarago ^{134, ID}, M. Vasileiou ^{77, ID}, A. Vasiliev ^{138, ID}, O. Vázquez Doce ^{95, ID},
 V. Vechernin ^{138, ID}, E. Vercellin ^{24, ID}, S. Vergara Limón ⁴³, L. Vermunt ^{57, ID}, R. Vértesi ^{134, ID},
 M. Verweij ^{57, ID}, L. Vickovic ³³, Z. Vilakazi ¹¹⁹, O. Villalobos Baillie ^{99, ID}, G. Vino ^{48, ID}, A. Vinogradov ^{138, ID},
 T. Virgili ^{28, ID}, V. Vislavicius ⁸², A. Vodopyanov ^{139, ID}, B. Volkel ^{32, ID}, M.A. Völk ^{94, ID}, K. Voloshin ¹³⁸,
 S.A. Voloshin ^{132, ID}, G. Volpe ^{31, ID}, B. von Haller ^{32, ID}, I. Vorobyev ^{95, ID}, N. Vozniuk ^{138, ID}, J. Vrláková ^{36, ID},
 B. Wagner ²⁰, C. Wang ^{38, ID}, D. Wang ³⁸, M. Weber ^{101, ID}, A. Wegrzynek ^{32, ID}, F.T. Weighofer ³⁷,
 S.C. Wenzel ^{32, ID}, J.P. Wessels ^{133, ID}, S.L. Weyhmiller ^{135, ID}, J. Wiechula ^{62, ID}, J. Wikne ^{19, ID}, G. Wilk ^{78, ID},
 J. Wilkinson ^{97, ID}, G.A. Willems ^{133, ID}, B. Windelband ^{94, ID}, M. Winn ^{126, ID}, W.E. Witt ¹¹⁸,
 J.R. Wright ^{106, ID}, W. Wu ³⁸, Y. Wu ^{116, ID}, R. Xu ^{6, ID}, A.K. Yadav ^{130, ID}, S. Yalcin ^{70, ID}, Y. Yamaguchi ^{92, ID},
 K. Yamakawa ⁹², S. Yang ²⁰, S. Yano ^{92, ID}, Z. Yin ^{6, ID}, I.-K. Yoo ^{16, ID}, J.H. Yoon ^{56, ID}, S. Yuan ²⁰,

A. Yuncu ^{94, ID}, V. Zaccolo ^{23, ID}, C. Zampolli ^{32, ID}, H.J.C. Zanolli ⁵⁷, F. Zanone ^{94, ID}, N. Zardoshti ^{32, 99, ID},
 A. Zarochentsev ^{138, ID}, P. Závada ^{60, ID}, N. Zaviyalov ¹³⁸, M. Zhalov ^{138, ID}, B. Zhang ^{6, ID}, S. Zhang ^{38, ID},
 X. Zhang ^{6, ID}, Y. Zhang ¹¹⁶, M. Zhao ^{10, ID}, V. Zherebchevskii ^{138, ID}, Y. Zhi ¹⁰, N. Zhigareva ¹³⁸, D. Zhou ^{6, ID},
 Y. Zhou ^{82, ID}, J. Zhu ^{97, 6, ID}, Y. Zhu ⁶, G. Zinovjev ^{3, I}, N. Zurlo ^{129, 53, ID}

¹ A.I. Alikhanyan National Science Laboratory (Yerevan Physics Institute) Foundation, Yerevan, Armenia

² AGH University of Science and Technology, Cracow, Poland

³ Bogolyubov Institute for Theoretical Physics, National Academy of Sciences of Ukraine, Kiev, Ukraine

⁴ Bose Institute, Department of Physics and Centre for Astroparticle Physics and Space Science (CAPSS), Kolkata, India

⁵ California Polytechnic State University, San Luis Obispo, CA, United States

⁶ Central China Normal University, Wuhan, China

⁷ Centro de Aplicaciones Tecnológicas y Desarrollo Nuclear (CEADEN), Havana, Cuba

⁸ Centro de Investigación y de Estudios Avanzados (CINVESTAV), Mexico City and Mérida, Mexico

⁹ Chicago State University, Chicago, IL, United States

¹⁰ China Institute of Atomic Energy, Beijing, China

¹¹ Chungbuk National University, Cheongju, Republic of Korea

¹² Comenius University Bratislava, Faculty of Mathematics, Physics and Informatics, Bratislava, Slovak Republic

¹³ COMSATS University Islamabad, Islamabad, Pakistan

¹⁴ Creighton University, Omaha, NE, United States

¹⁵ Department of Physics, Aligarh Muslim University, Aligarh, India

¹⁶ Department of Physics, Pusan National University, Pusan, Republic of Korea

¹⁷ Department of Physics, Sejong University, Seoul, Republic of Korea

¹⁸ Department of Physics, University of California, Berkeley, CA, United States

¹⁹ Department of Physics, University of Oslo, Oslo, Norway

²⁰ Department of Physics and Technology, University of Bergen, Bergen, Norway

²¹ Dipartimento di Fisica, Università di Pavia, Pavia, Italy

²² Dipartimento di Fisica dell'Università and Sezione INFN, Cagliari, Italy

²³ Dipartimento di Fisica dell'Università and Sezione INFN, Trieste, Italy

²⁴ Dipartimento di Fisica dell'Università and Sezione INFN, Turin, Italy

²⁵ Dipartimento di Fisica e Astronomia dell'Università and Sezione INFN, Bologna, Italy

²⁶ Dipartimento di Fisica e Astronomia dell'Università and Sezione INFN, Catania, Italy

²⁷ Dipartimento di Fisica e Astronomia dell'Università and Sezione INFN, Padova, Italy

²⁸ Dipartimento di Fisica 'E.R. Caianiello' dell'Università and Gruppo Collegato INFN, Salerno, Italy

²⁹ Dipartimento DISAT del Politecnico and Sezione INFN, Turin, Italy

³⁰ Dipartimento di Scienze MIFT, Università di Messina, Messina, Italy

³¹ Dipartimento Interateneo di Fisica 'M. Merlin' and Sezione INFN, Bari, Italy

³² European Organization for Nuclear Research (CERN), Geneva, Switzerland

³³ Faculty of Electrical Engineering, Mechanical Engineering and Naval Architecture, University of Split, Split, Croatia

³⁴ Faculty of Engineering and Science, Western Norway University of Applied Sciences, Bergen, Norway

³⁵ Faculty of Nuclear Sciences and Physical Engineering, Czech Technical University in Prague, Prague, Czech Republic

³⁶ Faculty of Science, P.J. Šafárik University, Košice, Slovak Republic

³⁷ Frankfurt Institute for Advanced Studies, Johann Wolfgang Goethe-Universität Frankfurt, Frankfurt, Germany

³⁸ Fudan University, Shanghai, China

³⁹ Gangneung-Wonju National University, Gangneung, Republic of Korea

⁴⁰ Gauhati University, Department of Physics, Guwahati, India

⁴¹ Helmholtz-Institut für Strahlen- und Kernphysik, Rheinische Friedrich-Wilhelms-Universität Bonn, Bonn, Germany

⁴² Helsinki Institute of Physics (HIP), Helsinki, Finland

⁴³ High Energy Physics Group, Universidad Autónoma de Puebla, Puebla, Mexico

⁴⁴ Horia Hulubei National Institute of Physics and Nuclear Engineering, Bucharest, Romania

⁴⁵ Indian Institute of Technology Bombay (IIT), Mumbai, India

⁴⁶ Indian Institute of Technology Indore, Indore, India

⁴⁷ INFN, Laboratori Nazionali di Frascati, Frascati, Italy

⁴⁸ INFN, Sezione di Bari, Bari, Italy

⁴⁹ INFN, Sezione di Bologna, Bologna, Italy

⁵⁰ INFN, Sezione di Cagliari, Cagliari, Italy

⁵¹ INFN, Sezione di Catania, Catania, Italy

⁵² INFN, Sezione di Padova, Padova, Italy

⁵³ INFN, Sezione di Pavia, Pavia, Italy

⁵⁴ INFN, Sezione di Torino, Turin, Italy

⁵⁵ INFN, Sezione di Trieste, Trieste, Italy

⁵⁶ Inha University, Incheon, Republic of Korea

⁵⁷ Institute for Gravitational and Subatomic Physics (GRASP), Utrecht University/Nikhef, Utrecht, Netherlands

⁵⁸ Institute of Experimental Physics, Slovak Academy of Sciences, Košice, Slovak Republic

⁵⁹ Institute of Physics, Homi Bhabha National Institute, Bhubaneswar, India

⁶⁰ Institute of Physics of the Czech Academy of Sciences, Prague, Czech Republic

⁶¹ Institute of Space Science (ISS), Bucharest, Romania

⁶² Institut für Kernphysik, Johann Wolfgang Goethe-Universität Frankfurt, Frankfurt, Germany

⁶³ Instituto de Ciencias Nucleares, Universidad Nacional Autónoma de México, Mexico City, Mexico

⁶⁴ Instituto de Física, Universidade Federal do Rio Grande do Sul (UFRGS), Porto Alegre, Brazil

⁶⁵ Instituto de Física, Universidad Nacional Autónoma de México, Mexico City, Mexico

⁶⁶ iThemba LABS, National Research Foundation, Somerset West, South Africa

⁶⁷ Jeonbuk National University, Jeonju, Republic of Korea

⁶⁸ Johann-Wolfgang-Goethe Universität Frankfurt Institut für Informatik, Fachbereich Informatik und Mathematik, Frankfurt, Germany

⁶⁹ Korea Institute of Science and Technology Information, Daejeon, Republic of Korea

⁷⁰ KTO Karatay University, Konya, Turkey

⁷¹ Laboratoire de Physique des 2 Infinis, Irène Joliot-Curie, Orsay, France

⁷² Laboratoire de Physique Subatomique et de Cosmologie, Université Grenoble-Alpes, CNRS-IN2P3, Grenoble, France

- ⁷³ Lawrence Berkeley National Laboratory, Berkeley, CA, United States
⁷⁴ Lund University Department of Physics, Division of Particle Physics, Lund, Sweden
⁷⁵ Nagasaki Institute of Applied Science, Nagasaki, Japan
⁷⁶ Nara Women's University (NWU), Nara, Japan
⁷⁷ National and Kapodistrian University of Athens, School of Science, Department of Physics , Athens, Greece
⁷⁸ National Centre for Nuclear Research, Warsaw, Poland
⁷⁹ National Institute of Science Education and Research, Homi Bhabha National Institute, Jatni, India
⁸⁰ National Nuclear Research Center, Baku, Azerbaijan
⁸¹ National Research and Innovation Agency - BRIN, Jakarta, Indonesia
⁸² Niels Bohr Institute, University of Copenhagen, Copenhagen, Denmark
⁸³ Nikhef, National institute for subatomic physics, Amsterdam, Netherlands
⁸⁴ Nuclear Physics Group, STFC Daresbury Laboratory, Daresbury, United Kingdom
⁸⁵ Nuclear Physics Institute of the Czech Academy of Sciences, Husinec-Řež, Czech Republic
⁸⁶ Oak Ridge National Laboratory, Oak Ridge, TN, United States
⁸⁷ Ohio State University, Columbus, OH, United States
⁸⁸ Physics department, Faculty of science, University of Zagreb, Zagreb, Croatia
⁸⁹ Physics Department, Panjab University, Chandigarh, India
⁹⁰ Physics Department, University of Jammu, Jammu, India
⁹¹ Physics Department, University of Rajasthan, Jaipur, India
⁹² Physics Program and International Institute for Sustainability with Knotted Chiral Meta Matter (SKCM2), Hiroshima University, Hiroshima, Japan
⁹³ Physikalisches Institut, Eberhard-Karls-Universität Tübingen, Tübingen, Germany
⁹⁴ Physikalisches Institut, Ruprecht-Karls-Universität Heidelberg, Heidelberg, Germany
⁹⁵ Physik Department, Technische Universität München, Munich, Germany
⁹⁶ Politecnico di Bari and Sezione INFN, Bari, Italy
⁹⁷ Research Division and ExtreMe Matter Institute EMMI, GSI Helmholtzzentrum für Schwerionenforschung GmbH, Darmstadt, Germany
⁹⁸ Saha Institute of Nuclear Physics, Homi Bhabha National Institute, Kolkata, India
⁹⁹ School of Physics and Astronomy, University of Birmingham, Birmingham, United Kingdom
¹⁰⁰ Sección Física, Departamento de Ciencias, Pontificia Universidad Católica del Perú, Lima, Peru
¹⁰¹ Stefan Meyer Institut für Subatomare Physik (SMI), Vienna, Austria
¹⁰² SUBATECH, IMT Atlantique, Nantes Université, CNRS-IN2P3, Nantes, France
¹⁰³ Suranaree University of Technology, Nakhon Ratchasima, Thailand
¹⁰⁴ Technical University of Košice, Košice, Slovak Republic
¹⁰⁵ The Henryk Niewodniczanski Institute of Nuclear Physics, Polish Academy of Sciences, Cracow, Poland
¹⁰⁶ The University of Texas at Austin, Austin, TX, United States
¹⁰⁷ Universidad Autónoma de Sinaloa, Culiacán, Mexico
¹⁰⁸ Universidade de São Paulo (USP), São Paulo, Brazil
¹⁰⁹ Universidade Estadual de Campinas (UNICAMP), Campinas, Brazil
¹¹⁰ Universidade Federal do ABC, Santo André, Brazil
¹¹¹ University of Cape Town, Cape Town, South Africa
¹¹² University of Houston, Houston, TX, United States
¹¹³ University of Jyväskylä, Jyväskylä, Finland
¹¹⁴ University of Kansas, Lawrence, KS, United States
¹¹⁵ University of Liverpool, Liverpool, United Kingdom
¹¹⁶ University of Science and Technology of China, Hefei, China
¹¹⁷ University of South-Eastern Norway, Kongsberg, Norway
¹¹⁸ University of Tennessee, Knoxville, TN, United States
¹¹⁹ University of the Witwatersrand, Johannesburg, South Africa
¹²⁰ University of Tokyo, Tokyo, Japan
¹²¹ University of Tsukuba, Tsukuba, Japan
¹²² University Politehnica of Bucharest, Bucharest, Romania
¹²³ Université Clermont Auvergne, CNRS/IN2P3, LPC, Clermont-Ferrand, France
¹²⁴ Université de Lyon, CNRS/IN2P3, Institut de Physique des 2 Infinis de Lyon, Lyon, France
¹²⁵ Université de Strasbourg, CNRS, IPHC UMR 7178, F-67000 Strasbourg, France, Strasbourg, France
¹²⁶ Université Paris-Saclay Centre d'Etudes de Saclay (CEA), IRFU, Département de Physique Nucléaire (DPhN), Saclay, France
¹²⁷ Università degli Studi di Foggia, Foggia, Italy
¹²⁸ Università del Piemonte Orientale, Vercelli, Italy
¹²⁹ Università di Brescia, Brescia, Italy
¹³⁰ Variable Energy Cyclotron Centre, Homi Bhabha National Institute, Kolkata, India
¹³¹ Warsaw University of Technology, Warsaw, Poland
¹³² Wayne State University, Detroit, MI, United States
¹³³ Westfälische Wilhelms-Universität Münster, Institut für Kernphysik, Münster, Germany
¹³⁴ Wigner Research Centre for Physics, Budapest, Hungary
¹³⁵ Yale University, New Haven, CT, United States
¹³⁶ Yonsei University, Seoul, Republic of Korea
¹³⁷ Zentrum für Technologie und Transfer (ZTT), Worms, Germany
¹³⁸ Affiliated with an institute covered by a cooperation agreement with CERN
¹³⁹ Affiliated with an international laboratory covered by a cooperation agreement with CERN

^I Deceased.^{II} Also at: Max-Planck-Institut für Physik, Munich, Germany.^{III} Also at: Italian National Agency for New Technologies, Energy and Sustainable Economic Development (ENEA), Bologna, Italy.^{IV} Also at: Dipartimento DET del Politecnico di Torino, Turin, Italy.^V Also at: Department of Applied Physics, Aligarh Muslim University, Aligarh, India.^{VI} Also at: Institute of Theoretical Physics, University of Wroclaw, Poland.^{VII} Also at: An institution covered by a cooperation agreement with CERN.